Contents

Chapter 3

Experiment, Results and Discussion

3.1 Preliminary Investigations

To study the properties of Cr_2O_3 thin films, it has to be investigated whether the material can be deposited via Pulsed Laser Deposition (PLD). Since α-Cr_2O_3 is the only phase of chromia (cf. 1.2.1), it is expected that the growth results in either rhombohedral or amorphous films. Furthermore, if a crystalline phase is present, the orientation with respect to the sapphire substrates is of interest. Because Al_2O_3 and Cr_2O_3 exhibit the same crystal symmetry, it is expected that the crystal orientation of the film matches the corresponding substrate orientation. Finally, deposition parameters should be optimized to obtain the best crystal quality.

3.1.1 Experiment

Due to the similar crystal structure of Cr_2O_3 and α-Ga_2O_3, the deposition parameters of the latter were chosen as a starting point to deposit chromia thin films on $10 \times 10\,\mathrm{mm}^2$ sapphire substrates with *m*-plane orientation. Namely, a pulse energy of 650 mJ and a pulse frequency of 20 Hz were applied for a total of 30 000 pulses. To investigate the influence of deposition parameters, three batches were produced:

1. variation of oxygen partial pressure from 8×10^{-5} to 1×10^{-2} mbar with a fixed temperature of 745 °C,

2. variation of growth temperature from 725 to 765 °C with a fixed oxygen partial pressure of 1×10^{-3} mbar, and

3. variation of substrate orientation between *c*- (00.1), *r*- (01.2) *m*- (10.0) and *a*-plane (11.0) $5 \times 5\,\mathrm{mm}^2$ sapphire substrates[1] with a fixed oxygen partial pressure of 1×10^{-3} mbar and a growth temperature of 715 °C.

Structural properties of those thin films were determined by 2ϑ-ω-scans, ω-scans and φ-scans. The thickness was determined via spectroscopic ellipsometry, and transmission spectra were recorded for two samples of the 1st batch to determine the optical band gap. Temperature dependent resistivity measurements were performed on the samples of the 3rd batch.

[1] In the following, the Bravais-Miller-indices will be omitted.

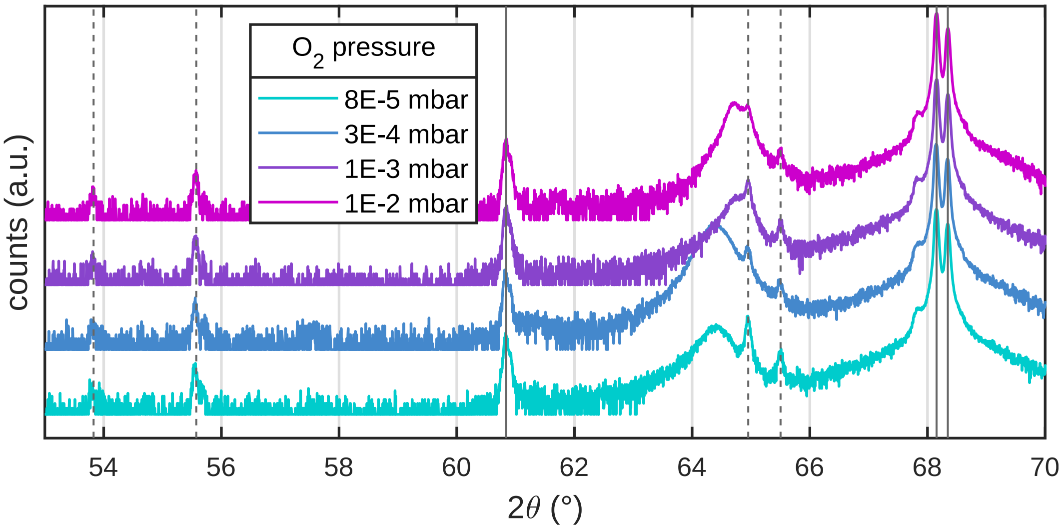

Figure 3.1: 2ϑ-ω-patterns of Cr_2O_3 thin films deposited on *m*-plane sapphire for various oxygen partial pressures. The solid lines indicate (30.0) substrate reflections corresponding to copper radiation, whereas the dashed lines indicate (30.0) substrate reflections corresponding to tungsten radiation.

3.1.2 Results

Oxygen Partial Pressure Variation on *m*-plane Sapphire

In the following, the results for the samples produced at four different oxygen partial pressures are analyzed. In Fig. 3.1, the 2ϑ-ω-patterns are depicted. For each pattern, the two peaks (solid line) at around 68° correspond to the (30.0) reflection of the *m*-plane oriented sapphire substrate. The splitting occurs due to the similar wavelength of Cu-Kα_1 and Cu-Kα_2 radiation. The additional peaks also stem mainly from the (30.0) reflection of Al_2O_3 and are caused by W-Lβ_2-, W-Lβ_1-, Cu-Kβ-, W-Lα_1- and W-Lα_2-radiation (increasing angles).[2] In the vicinity of the calculated peak position for the (30.0) reflection of Cr_2O_3 (cf. 1.3), there is a peak observed for each sample, indicating that the α-phase of Cr_2O_3 is present. Note that the peak position is varying depending on the chosen oxygen partial pressure. The difference to the expected peak position $2\theta_0$ is expressed as out-of-plane (o.o.p.) strain ϵ_{zz} using the Bragg equation Equ. 1.9 and then

$$\epsilon_{zz} = \frac{d - d_0}{d_0} = \left(\frac{1}{\sin(2\theta/2)} - \frac{1}{\sin(2\theta_0/2)}\right) \cdot \sin(2\theta_0/2)\,. \tag{3.1}$$

In Fig. 3.2a, the calculated strain is shown in dependence of the corresponding oxygen partial pressure. The strain decreases from approx. 0.95 % to 0.45 % with increasing pressure. This strain reduction may therefore be the result of increased background gas scattering which results in less kinetic energy of the specimen reaching the heated substrate (cf. 2.1.1).

For each sample, the 2θ angle was fixed to the observed (30.0) reflection of Cr_2O_3 and an ω-scan was performed. The Full Width at Half Maximums (FWHMs) of the ω-patterns (henceforth "ω-FWHM") are depicted in Fig. 3.2b. The values vary between

[2] **Klar wäre das besser das im plot an die linien zu schreiben, aber das war mir irgendwie zu auffändig es schön zu machen. Gehts auch so?**

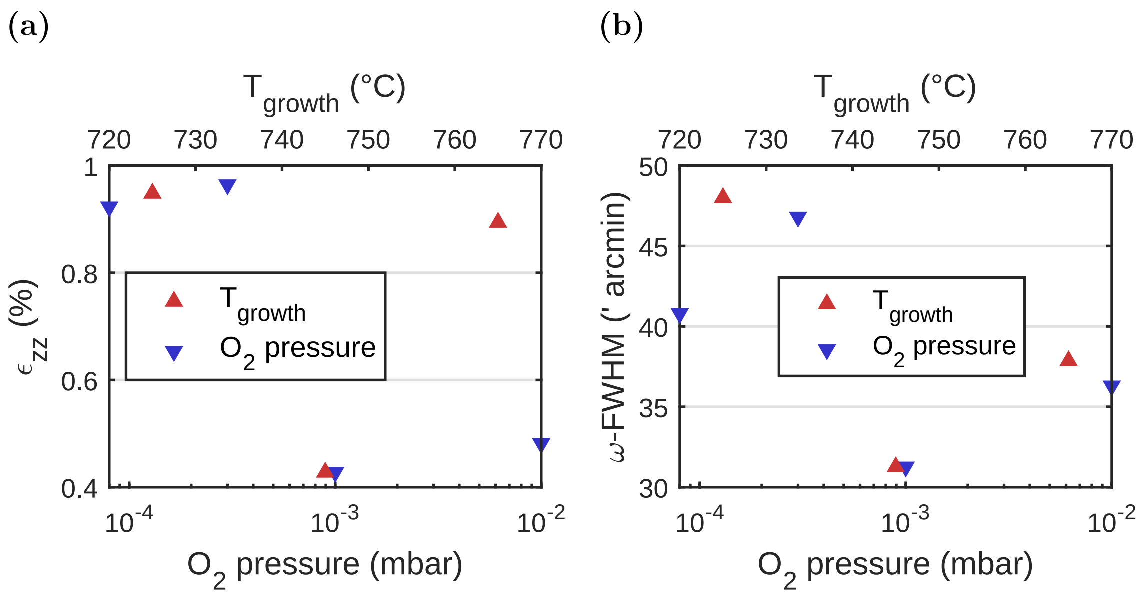

Figure 3.2: **(a)** o.o.p. strain calculated with Equ. 3.1 and **(b)** ω-FWHMs for samples from growth temperature series (red triangles, top x-axis) and oxygen partial pressure series (blue triangles, bottom x-axis).

approx. 30′ and 50′ and show a dependence on oxygen partial pressure, which is less pronounced compared with o.o.p. strain (Fig. 3.2a). Still, since ω-FWHM is connected to the mosaicity of the thin film, higher oxygen partial pressures yield slightly better crystal qualities.

To probe for rotational domains of the thin films, φ-scans were performed by fixing 2θ and ω to the corresponding angles of the (30.6) plane of Cr_2O_3, which has an inclination angle of 32.4° with respect to the (30.0) plane. The diffraction patterns are depicted in Fig. 3.3. The observed peaks of the thin film align with the peaks of the single crystal substrate, indicating that the film has no in-plane rotation with respect to the substrate. Furthermore, the absence of additional peaks indicates that there exists only a single domain of the thin film.

The growth rate g varies between 3 pm pulse^{-1} and 7 pm pulse^{-1} and is depicted in Fig. 3.4a. No systematic dependence on the oxygen partial pressure can be observed.

The transmission spectra of two selected Cr_2O_3 thin films are shown in Fig. 3.5a. The samples are not fully transparent in the visible spectrum and they exhibit a greenish tint, as can also be seen in Fig. 3.4b. To determine the onset of absorption E_τ, a Tauc-plot (Fig. 3.5b) is utilized (cf. **??**). The exponent is chosen to be $\frac{1}{2}$, resulting in a representation of $(\alpha E)^2$ vs. E. Although the publications used for reference in this work support the direct transition nature of Cr_2O_3 [1, 2], it has to be noted that there exist studies determining the optical band gap of Cr_2O_3 by applying an exponent of 2, assuming an indirect band gap transition for Cr_2O_3 [3, 4]. Fitting the linear regime in the onset of absorption results in $E_\tau \approx 3.7$ eV for both samples, which differ in strain and ω-FWHM by a factor of approx. 2 and 0.3, respectively.

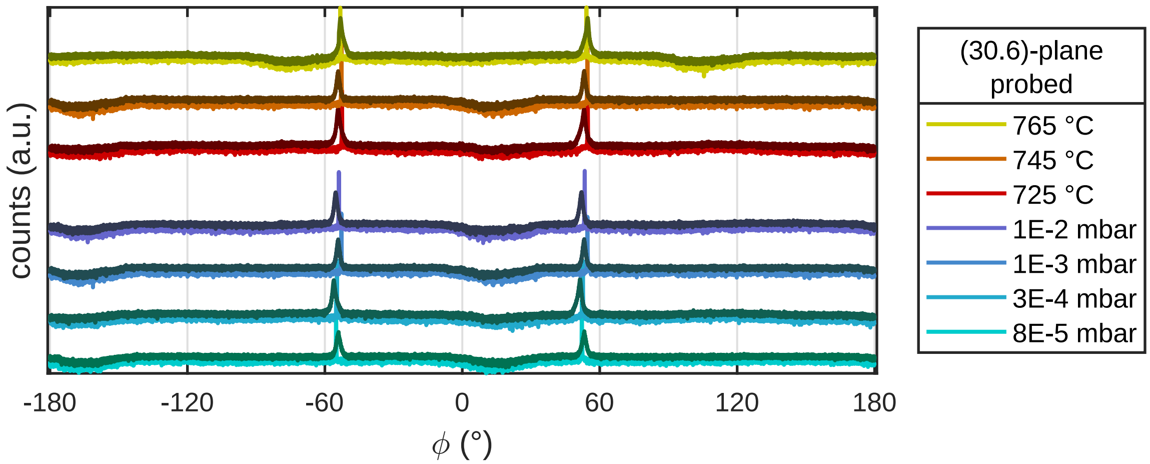

Figure 3.3: Diffraction patterns of φ-scans performed on the inclined (30.6) reflections for *m*-plane Cr_2O_3 (darker color) and Al_2O_3 (brighter color). The diffraction patterns cover the samples from variation of oxygen partial pressure (teal to blue colored) and variation of growth temperature (red to yellow colored).

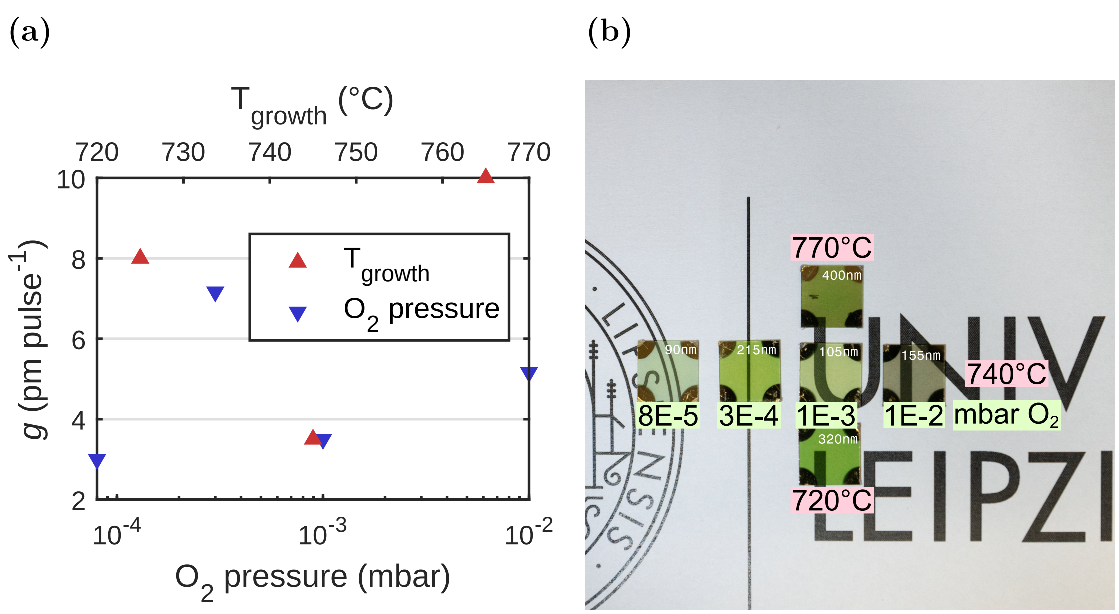

Figure 3.4: **(a)** Growth rates g for samples from growth temperature series (red triangles, top x-axis) and oxygen partial pressure series (blue triangles, bottom x-axis). **(b)** Image of the samples produced at different oxygen partial pressures and different growth temperatures.

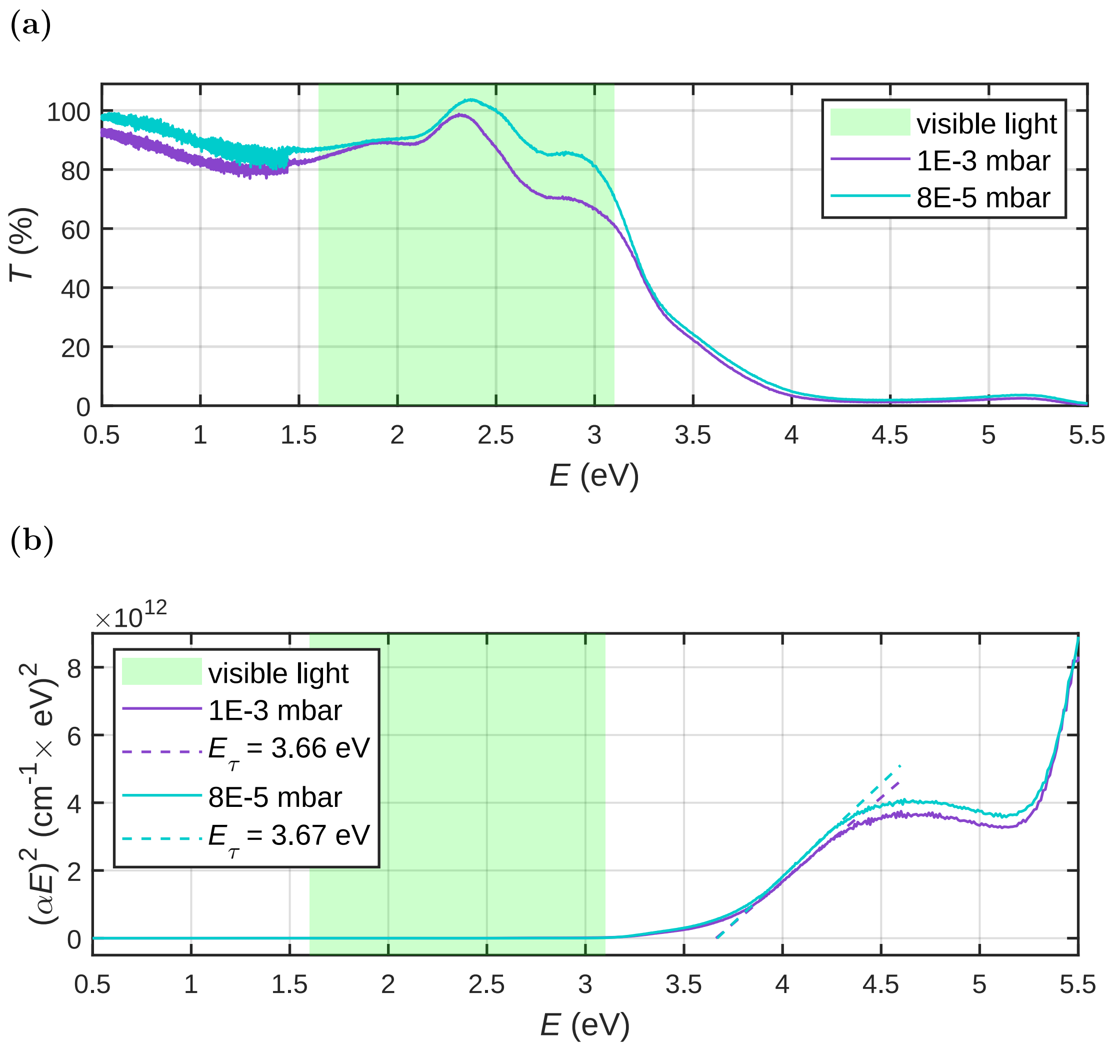

Figure 3.5: **(a)** Transmission spectra of two selected Cr_2O_3 thin films, deposited with different oxygen partial pressures. The spectra are normalized to a corresponding uncoated *m*-plane sapphire substrate. **(b)** Tauc-plot of the above-mentioned samples. It is assumed that Cr_2O_3 has a direct bandgap [1, 2].

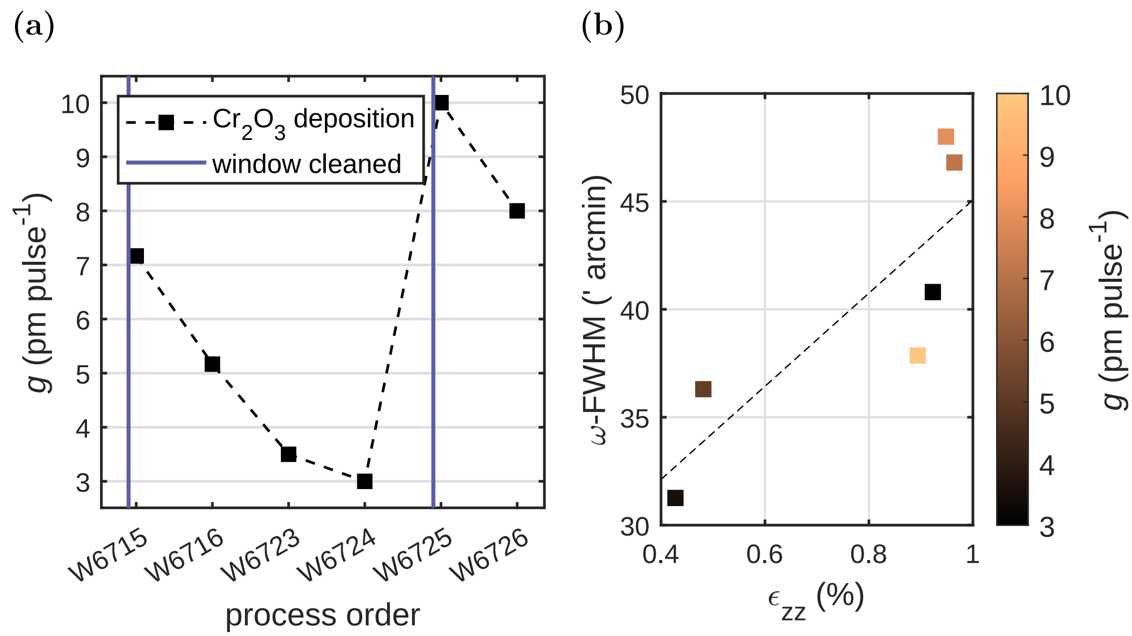

Figure 3.6: (a)

Growth Temperature Variation on *m*-plane Sapphire

In the following, the results for the three samples produced at different growth temperatures are presented. Similar to the previous results, the (30.0) reflection of the α-phase of Cr_2O_3 can be observed (Fig. 3.7). Note that the additional peaks are corresponding to the (30.0) reflection of the substrate and stem from various radiation wavelengths. The calculated o.o.p. strain is shown in Fig. 3.2a and a large spread of strain can be observed, varying between 0.4 % and 1 %. Note that there is no systematic dependence on growth temperature. The ω-FWHMs of the Cr_2O_3 (30.0) reflection are shown in Fig. 3.2b and exhibit a similar spread as the samples with varying oxygen partial pressure, but similar to the o.o.p. strain, no dependence on growth temperature is observed. The φ-scans (Fig. 3.3) show that the thin film is in-plane aligned with the substrate and that no rotational domains are present. Finally, the growth rate varies between 3.5 pm pulse^{-1} and 10 pm pulse^{-1} with no observable dependence on growth temperature.

Influence of Growth Rate on Crystal Structure

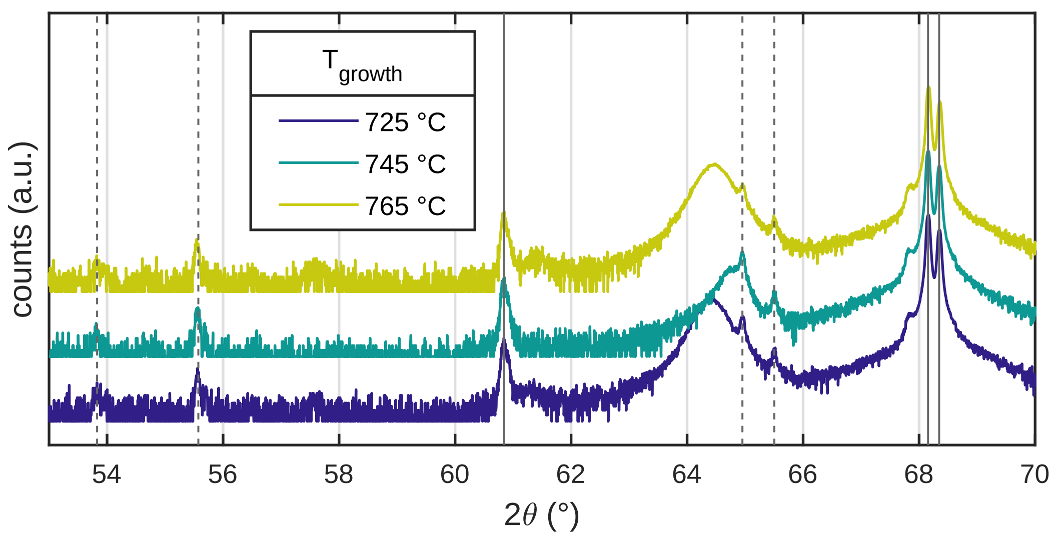

Figure 3.7: 2ϑ-ω-pattern of Cr_2O_3 thin films deposited on *m*-plane sapphire for three different growth temperatures. The lines indicate substrate reflections that stem from copper and tungsten radiation (cf. 3.1)

Bibliography

[1] L. Farrell et al. "Conducting mechanism in the epitaxial p-type transparent conducting oxide Cr_2O_3:Mg". In: *Physical Review B* 91.12 (2015), p. 125202. ISSN: 1098-0121, 1550-235X. DOI: 10.1103/PhysRevB.91.125202.

[2] Zhishan Mi et al. "The effects of strain and vacancy defects on the electronic structure of Cr_2O_3". In: *Computational Materials Science* 144 (2018), pp. 64–69. ISSN: 09270256. DOI: 10.1016/j.commatsci.2017.12.012.

[3] Chun-Shen Cheng, H. Gomi, and H. Sakata. "Electrical and Optical Properties of Cr_2O_3 Films Prepared by Chemical Vapour Deposition". In: *Physica Status Solidi (a)* 155.2 (1996), pp. 417–425. ISSN: 00318965, 1521396X. DOI: 10.1002/pssa.2211550215.

[4] M.F. Al-Kuhaili and S.M.A. Durrani. "Optical properties of chromium oxide thin films deposited by electron-beam evaporation". In: *Optical Materials* 29.6 (2007), pp. 709–713. ISSN: 09253467. DOI: 10.1016/j.optmat.2005.11.020.